Meta-Radiology 2 (2024) 100069

Contents lists available at ScienceDirect

Meta-Radiology

journal homepage: www.keaipublishing.com/en/journals/meta-radiology

Deep learning-based artificial intelligence for assisting diagnosis, assessment and treatment in soft tissue sarcomas

Ruiling Xu [a,b], Jinxin Tang [a,b], Chenbei Li [a,b], Hua Wang [a,b], Lan Li [d], Yu He [e], Chao Tu [a,b,c,*], Zhihong Li [a,b,c,*]

[a] Department of Orthopaedics, The Second Xiangya Hospital, Central South University, Changsha, China
[b] Hunan Key Laboratory of Tumor Models and Individualized Medicine, The Second Xiangya Hospital, Changsha, China
[c] Shenzhen Research Institute of Central South University, Guangdong 518063, China
[d] Department of Pathology, The Second Xiangya Hospital, Central South University, Changsha, China
[e] Department of Radiology, The Second Xiangya Hospital, Central South University, Changsha, China

ARTICLE INFO

Keywords:
Deep learning
Soft tissue sarcomas
Transfer learning
Generative adversarial network
Algorithm

ABSTRACT

Soft tissue sarcomas (STSs) represent a group of heterogeneous mesenchymal tumors of which are generally classified as per the histopathology. Despite being rare in incidence and prevalence, STSs are usually correlated with unfavorable prognosis and high mortality rate. Early and accurate diagnosis of STSs are critical in clinical management of STSs. Deep learning (DL) refers to a subtype of artificial intelligence that has been adopted to assist healthcare professionals to optimize personalized treatment for a given situation, particularly in image analysis. Recently, emerging studies have demonstrated that application of DL based on medical images could substantially improve the accuracy and efficiency of clinicians to the identification, diagnosis, treatment, and prognosis prediction of STSs, and thereby facilitating the clinical decision-making. Herein, we aimed to extensively summarize the recent applications of DL-based artificial intelligence in STSs from the aspects of data acquisition, algorithm, and model establishment. Besides, the reinforcement of the model by transfer learning and generative adversarial network (GAN) for data augmentation has also been elaborated. It is worth noting that high-quality data with accurate annotations, as well as optimized algorithmic performance are pivotal in the clinical application of DL in STSs.

1. Introduction

Soft tissue sarcomas (STSs) are a rare and highly diverse group of solid tumors that develop from mesenchymal precursor cells.[1,2] It includes a broad range of malignancies of soft tissues with distinct biological behavior and clinical outcome.[3] Currently, 137 types of STSs have been annotated,[4] but only account for approximately 1% of all new malignancies in adults.[5] The outcome of these patients has been unfavorable despite the development of several novel therapies or combinations of chemotherapy.[5,6] It is reported that patients with distant metastasis have an overall survival less than 16 months.[6] Therefore, for risk assessment and management strategies, early and accurate diagnosis of STSs and stratification of tumor grades are crucial.

Recently, As a field of artificial intelligence (AI), deep learning (DL) has emerged as a powerful statistical tool for dealing with a range of real-life problems,[7] including computer vision,[8] speech recognition,[9] natural language processing (NLP),[10] reinforcement learning[11] and others.[12,13] Currently, multiple DL models have been developed based on radiographic images, such as X-rays,[14,15] CT,[16] and MRI.[17] Besides, DL applications have also been observed in diagnostic pathology involving histopathological images.[18,19] Emerging studies were designed specifically for HE-stained images and demonstrated a profound impact on diagnoses.[17,20,21] Notably, the application of DL is evolving in all areas of medicine, including electrocardiographic,[22,23] brain disease,[24,25] traumatology,[23,26–28] and drug discovery.[29] Recently, DL-based AI is emerging in tumors, including breast cancer,[30,31] lung cancer,[32,33] colorectal cancer,[34] gastric cancer,[35] prostate cancer,[36] cervical cancer,[37] thyroid cancer,[38] and bone tumor. For instance, it has been shown that DL can distinguish benign bone lesions from malignancies, thus assisting in bone tumor differentiation.[39]

* Corresponding author. Department of Orthopaedics, The Second Xiangya Hospital, Central South University, No. 139 Renmin Road, Changsha, Hunan 410010, China.
E-mail addresses: tuchao@csu.edu.cn (C. Tu), lizhihong@csu.edu.cn (Z. Li).

https://doi.org/10.1016/j.metrad.2024.100069
Received 12 December 2023; Received in revised form 18 February 2024; Accepted 26 February 2024
Available online 29 February 2024

Though being relatively rare compared to other tumors, STSs have shown a steady increase in occurrence in the past decade and are associated with a high mortality rate.[40–42] Of note, young people are at risk especially for certain subtypes of STSs, which may contribute to a significant portion of the deaths.[43] It is pivotal to classify these tumors accurately due to their unique biological properties, prognosis, and treatment strategies. Medical images are important in the management of STSs, but the diagnostic expertise requires a long learning curve and is often limited to a few medical centers.[40] More recently, several methods of AI and configurations have been applied to STSs as well,[40,44] indicating DL in the identification, diagnosis, treatment, and prognosis of STSs could greatly improve the accuracy and efficiency of clinicians, as shown in Fig. 1. Herein, this review aimed to summarize the recent advancement in the application of DL-based AI in STSs and hope to shed light on the research in this emerging field.

2. Application of DL-based AI in STSs

2.1. Data acquisition and processing

Classification has been performed using DL based on the training dataset and learning algorithms to discover hidden patterns and structures.[45] The diagnosis of STSs should incorporate clinical manifestations, radiographic images (X-ray, CT, and MRI), and pathological examination.[46] Given the complexity of tumor biology, sometimes the data of multi-omics need to be jointly analyzed. Using multi-model data, including radionics, genomics, transcriptomics, metabolomics, and clinical factors, to describe a tumor landscape more accurately and thereby improve the diagnostic accuracy. At present, most researchers obtain data through multi-center images,[47–52] or combined with resources from public databases, such as TCGA,[40,53] and SEER (Surveillance, Epidemiology, and End Results), and the clinical data will also be included in the model establishment.[54,55] It should be noted that the original data (clinical data, image data, etc.) needs a critical data preprocessing step. Deep learning may benefit from data whitening and normalization as they reduce the impact of non-normalized data.[56] The preprocessing of image data is complex. Therefore, various methods are adopted in image processing, including image normalization, augmentation, shape augmentation, color augmentation, annotation, and segmentation.[57]

Among these processes, annotation and segmentation are key steps.[58,59] Investigators have observed the following remarkable characteristics in image segmentation: Generally, image segmentation using one algorithm alone is unsatisfactory, it therefore required a combination of multiple algorithms to achieve satisfactory results.

Besides, although studies have attempted to automatically identify and segment lesions or regions of interest (ROI), the results are usually below expectation, which may be attributed to the complexity of anatomical structures.[60] Since the location of STSs varies in the human body, which may introduce much difficulty in segmentation and annotation compared with other tumors like brain tumors or lung cancers, it is still necessary to perform these tasks manually in STSs.

2.2. Deep learning algorithm

DL algorithms are often referred as neural networks, and these algorithms could combine with multiple features into further strategies.[61] The successful application of DL algorithms that are trained on large amounts of data with annotation, has been demonstrated in tumor detection and classification.[62]

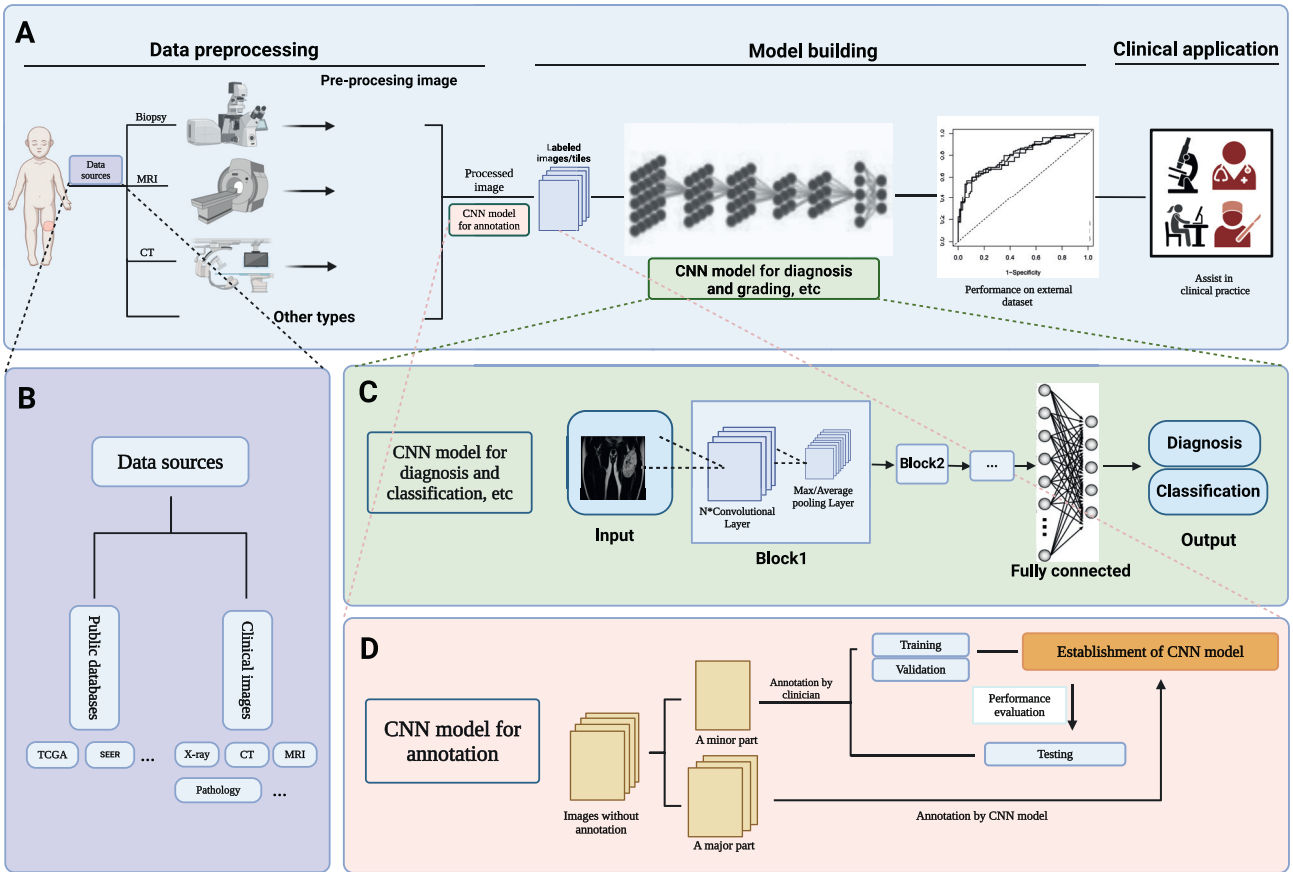

Fig. 1. Establishment of CNN model in STSs. (**A**) Process of deep learning model building, (**B**) access to data sources, (**C**) flow chart of establishing a deep learning model for diagnosis and classification, (**D**) and establishing a deep learning model for segmentation and annotation.

An artificial neural network (ANN) is formally summarized into three layers: input layer, hidden layer, and output layer. Many early diagnostic models used CNN architecture. The full connection layer downstream of CNN is similar to the ANN, but CNN allows color images to be used as input data.[63] A layer on the input passes information to several hidden layers which are activated based on the input and feed this information to the layer on the output, reflecting the class that was assigned.[64] Convolution layers, pooling layers, and fully connected layers are usually included in hidden layers. Convolution layers help extract characteristics from input data.[65] The pooling layers are generally located behind the convolution layers. The amount of information can be compressed by reducing the dimension of the input data to avoid overfitting.[66] Finally, these features are fed to some fully-connected layers for classification.[66] Different requirements could adjust the structure of CNN accordingly. For example, only feature extraction is needed for subsequent machine learning (ML), and the full-connection layer is not needed.[44]

2.2.1. Development of CNN models

CNN models have undergone many changes. This section mainly introduces the evolution of several models commonly used (Fig. 2).

LeNet was launched in 1998, laying a foundation for future image classification research using CNNs.[67] Although LeNet has achieved good results and demonstrated the potential of CNN, its computing power and data volume were insufficient. In 2012, AlexNet was proposed to address this challenge. It defined the actual classification network framework in the next decades: convolution, ReLu nonlinear activation, combination of MaxPooling and Dense layer. Inception V1, proposed in 2014, used a 22-layer structure to break through the limitation of network depth.[68] Furthermore, Simonyan K et al. proposed the visual geometry group (VGG) model in 2015.[69] It not only used a deeper network, but also reduced computing costs while achieving better performance. These studies demonstrated that further deepening was indeed the right direction to improve accuracy. Residual neural network (ResNet) was proposed in the same year, adding a residual block to the output.[70] It also borrowed bottlenecks and batch processing standardization from the Inception network. In 2016, dense convolutional network (DenseNet) further expanded the idea of ResNet.[71] It not only provided skip connections between layers, but also had skip connections from all previous layers.

Nowadays, many other models are still evolving. The algorithms can be selected according to different purposes. In STSs, most researchers will compare several improved models and adopt the best one for clinical application.

2.2.2. CNN models applied in STSs

Algorithms for identifying target features in STSs have been developed steadily. An overview of the algorithms used in STSs and its advantages were depicted below (Table 1).

AlexNet was applied to the classification of rhabdomyosarcoma (RMS), and ReLU was used as an activation function for the first time.[72] In the last layer of softmax classification, the number of output nodes has changed to improve the accuracy of classification.[49] Compared with Alexnet, ResNet can provide a method to solve the problem of gradient disappearance by using deep residual network.[73] ResNet architecture with different layers was widely used in soft tissue sarcomas. ResNet18 was used to predict the probability of anoxia in each pixel.[74] ResNet34 was used to predict lung metastasis of STS,[75] and ResNet50 was used to automatically extract DL features.[76] Moreover, DenseNet has the advantage of a narrower network and fewer parameters, which is largely due to the design of this deny block. Accordingly, Navarro et al.[51] choose DenseNet as their DL strategy for tumor grading after comparing with other architectures, including AlexNet, ResNet, VGGNet, WideResNet, and CBRNet.

According to Ronneberger et al.[77] experience, Holbrook et al. have implemented a 3D fully convolutional U-net network to segment STSs in mice.[78] U-net is improved based on a full CNN (FCN), and data augmentation can be used to train some data with relatively few samples. Furthermore, an approach for predicting gross tumor volume (GTV) confidence maps was developed by T. Marin et al., which was also based on U-net. By combining contracting and expanding paths with skip connections, the U-net architecture captures spatial data.[79] Importantly, several techniques were further used to improve the U-net architecture. For instance, the use of a 2.5D U-net could minimize memory requirements and make small training data available, and self-taught attention maps make the proposed network less susceptible to class inequality. Similar to U-net, fewer parameters are needed and the model can be computed more quickly by using the InceptionV3 model.[80]

Interestingly, the detection and localization of objects within images can be accomplished using few DL architectures at the moment, such as RCNNs and faster-RCNNs,[81] single shot multi-box detectors (SSDs),[82] and YOLO (you're only looking once).[83] Due to its excellent performance, T. Zehra et al. evaluated all object detection algorithms and selected YOLOv4 as a baseline to detect mitoses automatically in uterine leiomyosarcoma (LMS). Besides, many other studies also confirmed that YOLOv4 is superior to other algorithms for detecting objects.[84–86]

2.3. Establishment of model and clinical application

2.3.1. Recognition and classification

There is a relatively low incidence of STSs, which are characterized by low-to-high levels of aggression based on its grading scale.[87] The assessment of patient survival risk and the selection of therapeutic options must therefore be based on tumor grading prior to treatment.[88] The popular databases that can be used in the establishment of STSs deep learning model are shown in Table 2.

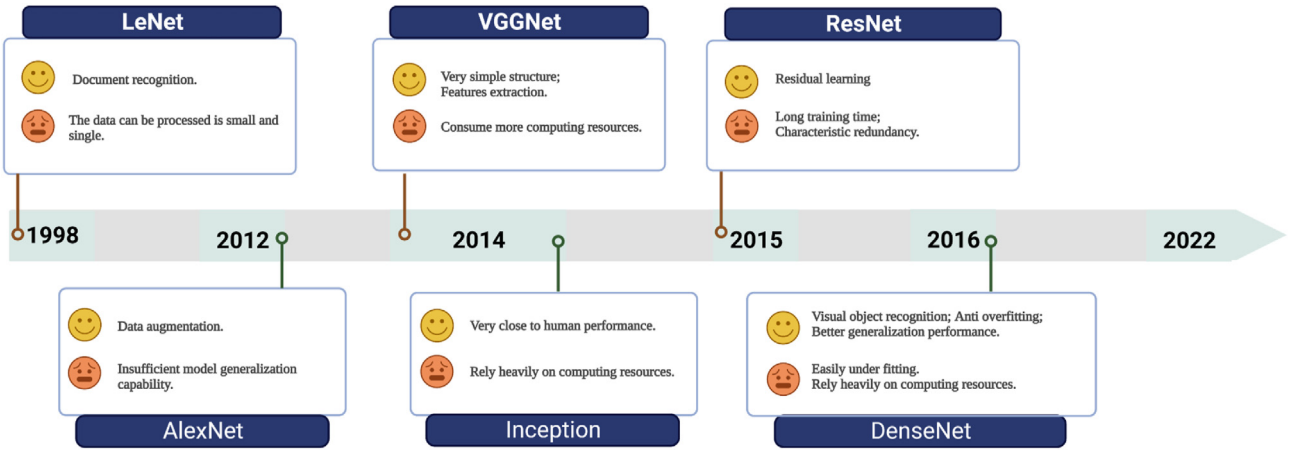

Fig. 2. Timeline for development of several CNN models.

Table 1
Summary of clinical studies involving deep learning in STSs.

Ref.	Tumors	Modality	Algorithm	Performance (metric)	Conclusion
[49]	RMS	MRI	AlexNet	85% cross validation prediction accuracy	Differential diagnosis of embryonal and alveolar RMS
[51]	STSs	MRI	DenseNet-161	The T1FSGd (AUC 0.75) and T2FS (AUC 0.76)	Predicting tumor grading
[44]	STSs	MRI	ResNet34	C index≥ 0.721, median AUC ≥0.746, and integrated Brier score ≤0.159	Predicting STSs recurrence
[40]	STSs	Histopathological slides	DenseNet121	AUC 0.97, accuracy, 0.799	Diagnose frequent subtypes of STSs
[139]	STSs	PET-CT	Multi-modality collaborative learning	AUC 0.8438, accuracy 0.8542, sensitivity 0.9167	Predict the distant metastases of STSs
[50]	STSs	DWI	VGG-19	training and validation accuracies were 86.5% and 84.8%.	Predict the pathologic treatment effect from longitudinal DWI
[52]	STSs	OCT	ResNet-50	accuracy 97.1%, sensitivity 94.3%	Assist clinicians in detecting the specific location of a lesion
[47]	SS	Clinical information	SNN	In fivefold cross validation was 0.87 in the survival neural network.	Predict survival of patients accurately
[55]	GU-RMS	Clinical information	DNN	The AUC 0.93 for 5-year overall survival and 0.91 for disease-specific survival.	Prediction of pediatric GU-RMS survival
[102]	RMS	Histopathological slides	InceptionV3	The RMS classification model (AUC >0.92)	Subtype classification and prognosis prediction for RMS
[106]	ULMS	Histopathological slides	YOLOv4	Model detection for mitosis (0.7462 precision, 0.8981 recall, and 0.8151 F1-score)	Mitotically active regions can be detected
[103]	RMS	Histopathological slides	DeepPATH CNN software suite	The RMS classification model (AUC >0.889)	Subtype classification
[140]	Sarcomas	CT	U-Net	Dice score was 87% and the Hausdorff distance was 14 mm	Predict accurate contours
[76]	LPS	CT, MRI	ResNet50	AUC 0.942, accuracy 0.86, sensitivity 0.95, specificity 0.77	Differentiate WDLPS from lipomas
[75]	STSs lung metastasis	MRI	ResNet34	AUC 0.833	Lung metastasis-status prediction in STSs
[133]	Solid and hematologic malignant neoplasms	DNA methylation	MethylationToActivity	Highly accurate and robust in revealing promoter activity landscapes	To infer promoter activities based on H3K4me3 and H3K27ac enrichment

Abbreviations: AUC: Area under curve; CNN: Convolutional neural network; DLRN: Deep learning radiomic nomogram; DNN: Deep neural networks; DWI: Diffusion-weighted MRI; GU-RMS: Genitourinary rhabdomyosarcoma; LPS: liposarcoma; MRI: Magnetic resonance imaging; PET-CT: Positron emission tomography-computed tomography; RED_SNN: Risk estimate distance survival neural network; RMS: rhabdomyosarcoma; ROI: Region of interest; SS: Synovial sarcoma; STSs: Soft tissue sarcomas; ULMS: Uterine leiomyosarcoma; WDLPS: Well-differentiated liposarcoma.

Table 2
Summary of popular databases involving deep learning STS diagnosis and treatment.

Database	Country/Region	Data type
The Cancer Imaging Archive (TCIA)	America	CT/MRI/Digital histopathology
MedPix	America	CT/MRI
Global Burden of Disease (GBD)	America	Prevalence of disease
The Surveillance, Epidemiology, and End Results (SEER)	America	Cancer prognosis
Orphanet	Europe	Medication for rare diseases
The Cancer Genome Atlas Program (TCGA)	America	Cancer genome

A CNN model was developed to automatically classify the histopathological subtypes of RMS.[49] The model fused MR images from seven females and fourteen males, which can be used for differential diagnosis of embryonal and alveolar subtypes of RMS. MR images were classified according to RMS type, and 85% accuracy was obtained. After testing, the classification accuracy of the system reached 95%.[49] However, this study had several limitations, one of which was the small number of cases, which increased the risk of overfitting the model to the training dataset. However, it is worth noting that transfer learning was applied to the model building. Traditional ML assumes that training data and testing data are sourced from the same domain, but no data is usually available in this area. Therefore, there is a need to create high-performing learners trained with data obtainable from different domains, and the methodology which addresses this need is called transfer learning (Fig. 3).[89] In addition, MRI and transfer learning technology were also used to low-grade (G1) and high-grade (G2/G3) STSs non-invasively. The DenseNet 161 architecture was used to develop DL models based on transfer learning. Overall, AUC values of 0.75 and 0.76 were achieved in the testing cohort, for the T1 and T2-weighted fat-saturated-based DL models, respectively.[51]

Radiation therapy is now well-established as an effective treatment for STSs with close margins or those prone to local recurrence before surgery.[90] It is essential to define the GTV accurately before radiotherapy can be effective. In certain cases, however, the GTV definition can be time-consuming and inaccurate, as it depends largely on the quality of the CT simulation.[91,92] Recently, an automatic drawing of GTV contours of STSs from CT images was developed based on a DL model. In this study, 87% of the predicted confidence maps matched the true confidence maps in a continuous Dice test. Accordingly, this method was capable of predicting contours accurately while utilizing variability and can thus improve clinical workflow. Meanwhile, Marin et al. proposed a framework using DL to automatically segment GTV.[93] Moreover, the researchers developed multimodality DenseNet, which could be applied even in radiation therapy of pan-cancers, including sarcomas and lung cancers.

2.3.2. *Pathological diagnosis*

Currently, the pathology practice is still heavily reliant on analog technologies such as conventional benchtop microscopes, glass slides, and written reports, while other disciplines have already experienced almost complete digitalization.[40] A commercially available scanning solution allows scanning H&E-stained microscopical slides to create digital histopathology.[94] Therefore, automation of diagnostic systems may be possible through the development of DL models based on digital histopathology. Recently, the effectiveness of DL algorithms in identifying patterns in whole-slide images (WSI) of STSs has also been demonstrated as well.[95–98]

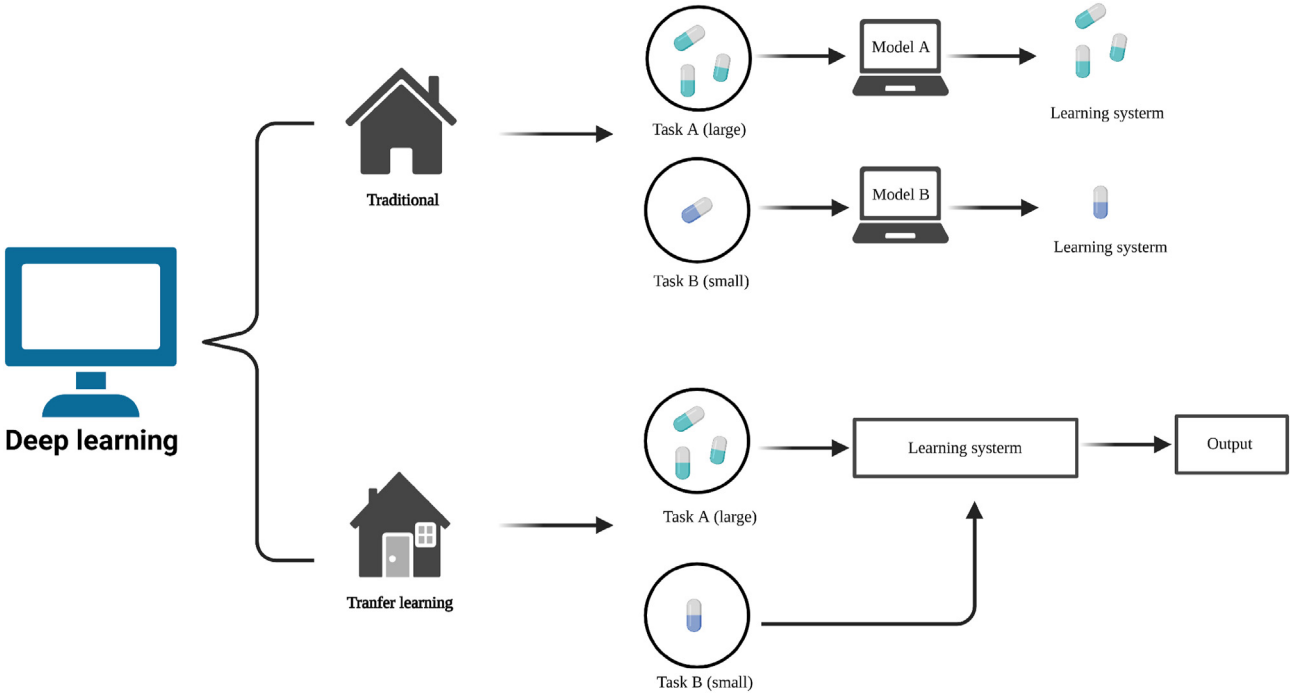

Fig. 3. Schematic diagram of transfer learning.

RMS is the most frequent malignant STSs in children,[99] which has several histological subgroups that influences patients' treatment and prognosis.[100,101] Pathologists need assistance with histological classification, biomarkers of IHC, or even next-generation sequencing (NGS) data to make better predictions. Through the use of digital pathological images, a model has been performed that can accurately classify RMS histological subtypes for auxiliary diagnosis.[102] The training data and testing data included 10,658 and 1674 patches, respectively, showing an accuracy of 87.9% for the RMS classification. Additionally, a prognostic model was further developed by enrolling embryonal RMS patients, which could distinguish high-risk from low-risk patients with significant differences in event-free survival outcomes ($p = 0.02$) in the testing data set. Similarly, another study used DeepPATH software to create a CNN model to distinguish alveolar RMS, embryonal RMS, and clear-cell sarcoma tumor.[103]

As a common invasive uterine sarcoma, uterine LMS often has a poor prognosis and can be difficult to diagnose.[104] The current methodology used by pathologists for diagnosing and grading uterine LMS is mainly based on mitosis count, necrosis, and nuclear atypia.[105] A biomarker of importance and challenge is the mitosis count. Recently, a DL-based automated mitosis detection algorithm for uterine LMS was presented by T. Zehra et al.[106] The training set contained 240 mitoses, while the testing images contained 108 mitoses. Based on the experimental results, the precision, recall, and F1 score of the test were 0.7462, 0.8981, and 0.8151, respectively. Based on these preliminary results, DL may be a promising approach for detecting mitotically active regions in uterine LMS.

More recently, Foersch S et al. conducted a multicentered study using 506 histopathological slides from 291 STSs patients,[40] including a TCGA cohort (240 patients) and a multicenter cohort (51 patients) in several centers. The former served as a training set, while the latter serves as a testing set. With a DL model based on standard DenseNet121, ROC values and diagnostic accuracy for the five most common STSs subtypes, including dedifferentiated liposarcoma (DDLPS), LMS, myxofibrosarcoma (MFS), synovial sarcoma not otherwise specified (SS), and undifferentiated pleomorphic sarcoma (UPS), averaged 0.97 and 0.799, respectively. A significant improvement was noted in the accuracy of pathologists from 0.46 to 0.84, implicating that DL can accurately diagnose frequent subtypes of STS and assist clinicians to make faster and more precise decisions.[40]

Importantly, a pathologist can also determine patients' response to chemotherapy by evaluating resected tumor specimens after adjuvant therapy to identify the risks of individuals to improve their outcomes.[107] However, this process can be time-consuming. The combination of DL with WSI may offer a promising and valuable strategy for this issue. However, several questions should be addressed before automating the analysis of histology images. Due to the complexity and diversity of image data, and the large size of individual histology slides, computing tasks can be pretty complex and require more computation power.[108] Meanwhile, the problem of overfitting is also challenging.[17]

2.3.3. *Prognosis prediction*

In addition to the assessment and classification of STSs, some studies adopted the DL model to study prognosis and recurrence as well.

To target anti-hypoxia-resistant habitats, hypoxia-activated prodrugs (HAPs) have been developed.[109] Sarcoma preclinical and early clinical trials have been performed to demonstrate the efficacy of HAP evofosfamide (TH-302).[110] However, TH-302 was found not successful in improving survival in phase III clinical trials when combined with doxorubicin (DOX),[111] which may be attributed to the absence of evaluation for stratification of hypoxic status. Thus, a DL model was developed by BV Jardim-Perassi et al. to identify hypoxia in patients so that HAPs could be better prescribed to them.[74] Interestingly, a strong correlation was found between the true hypoxia score in histology and the predicted in multiparametric pre-therapy MRI images using the DL model. Besides, in the hypoxic patient-derived xenograft model, TH-302 monotherapy or combined with DOX prolonged survival, suggesting DL models based on MRI can be used to monitor HAPs therapy response and forestall the occurrence of resistance.

Besides, in order to predict the response of STSs to radiotherapy by longitudinal diffusion-weighted MRI (DWI), Gao Y et al. used DL and generative adversarial network (GAN)-based data augmentation to develop a novel prediction framework for response prediction.[50] GAN is a type of deep learning model that consists of two parts: a generator that learns to generate plausible data, and a discriminator that learns to distinguish between real and fake data. The generator takes as input a

fixed-length random vector and learns to produce samples that mimic the distribution of the original dataset, while the discriminator then classifies the generated samples as "real" or "fake". When there is a limited amount of training data available or when the dataset is imbalanced, by training the generator and discriminator together, GAN can generate realistic synthetic data that can be used to improve the performance of deep learning models (Fig. 4). Because in some classification targets, the number of rare disease subtypes in training set may be small or even missing, which is very unfavorable for training DL models. Despite performing well in most disease detection tasks; DL techniques are less successful when categorizing rare disease subtypes. Due to the poor generalization ability of the techniques, they have difficulty in fitting the model. In order to increase the training data for DL-based computer--assisted diagnosis systems, GAN-based data augmentation is a solution to the data hunger of this kind of training set.[112,113] GAN can be used in a wide variety of medical applications in image synthesis. In addition to conventional MRI and CT images,[114] other medical images, including slit lamp images,[115] fluoroscopic images,[116] and photos of skin lesions, could also be incorporated in GAN for data analysis.[117]

To augment the data size, an auxiliary classifier GAN (ACGAN) was trained on 20 patients.[50] Training the model using synthetic data was followed by verification and testing with samples from five patients. The average accuracy of training and verification exceeded 84%, indicating that the generated samples could represent the original patient data. In the testing dataset, the accuracy of layer-by-layer prediction was greater than 80%. One round and six rounds of patient-based prediction resulted in 80% and 100% accuracy, respectively.[50] It should be noted that there have been a growing number of studies on the application of this novel method of generating images by DL to train models in diseases such as fractures and joint degenerative diseases,[118,119] but there are few studies concerning the STSs. More studies on application of GAN in STSs may be explored in near future.

In large patient data sets, ML offers the ability to identify patterns that would otherwise be unintuitive, which allows for the analysis of complex data.[54] An effective survival model, Cox proportional hazard regression (CoxPHR) has been shown to predict the survival time of multiple tumors accurately. However, conventional prediction models perform poorly at predicting rare malignancies.[47] Recently, a new DL-based prediction model based on 242 patients was developed. After comparing with traditional CNNs and Cox regression models,[47] the AUC of the survival neural network reached a median value of 0.87 in fivefold cross-validation, which is significantly higher than 0.792 for the simple neural network. In addition, SEER database was also used to develop a deep survival neural network model to predicting the survival rate of patients with spine-pelvic chondrosarcoma.[54] 80% of patients were used as training sets and the rest as testing sets. To interpolate missing values, k nearest neighbor was used. This model was based on the idea that events and time should be viewed as two distinct dimensions and that the CNN used a multimodal algorithm to learn these two objectives simultaneously. Similarly, an algorithm for predicting the 5-year survival rate of children with genitourinary RMS was also based on SEER database, including 277 patients[55] An 8/2 split of the dataset was used for training and testing deep neural networks (DNNs) as part of a five-fold cross--validation method. According to the DNN models, AUC was 0.93 for overall survival and 0.91 for disease-specific survival, both outperformed than those of the Cox proportional hazards (CPH) models, indicating that DL may provide better prognosis prediction for patients with rare malignancies than multivariable CoxPHR models.[55] Collectively, these studies suggest that DL approaches may help to predict patient outcomes.

2.3.4. *Combination of DL and radiomics*

The combination of traditional radiomics and DL is also a field worth exploring, through which we could benefit from both advantages.[120] Feature extraction is one of the key steps of the radiomic process.[121] Combining the features extracted by DL with those by radiomics to establish a prediction risk model is a method adopted by some researchers.[44,122]

The model was successfully established to predict the tumor grade and clinical outcome by combining manually extracted the features of radiomics and automatically extracted the characteristics of DL.[122] When compared with other prediction models, these models showed superior prognostic capabilities with diminished errors. Remarkably, this study also compared prediction models, and the DL radiomics nomogram (DLRN) has been shown to be a useful tool for predicting STSs recurrence.

As mentioned above, patients with STSs who have distant metastases have a poor prognosis.[123] The DLRN model was designed to predict lung

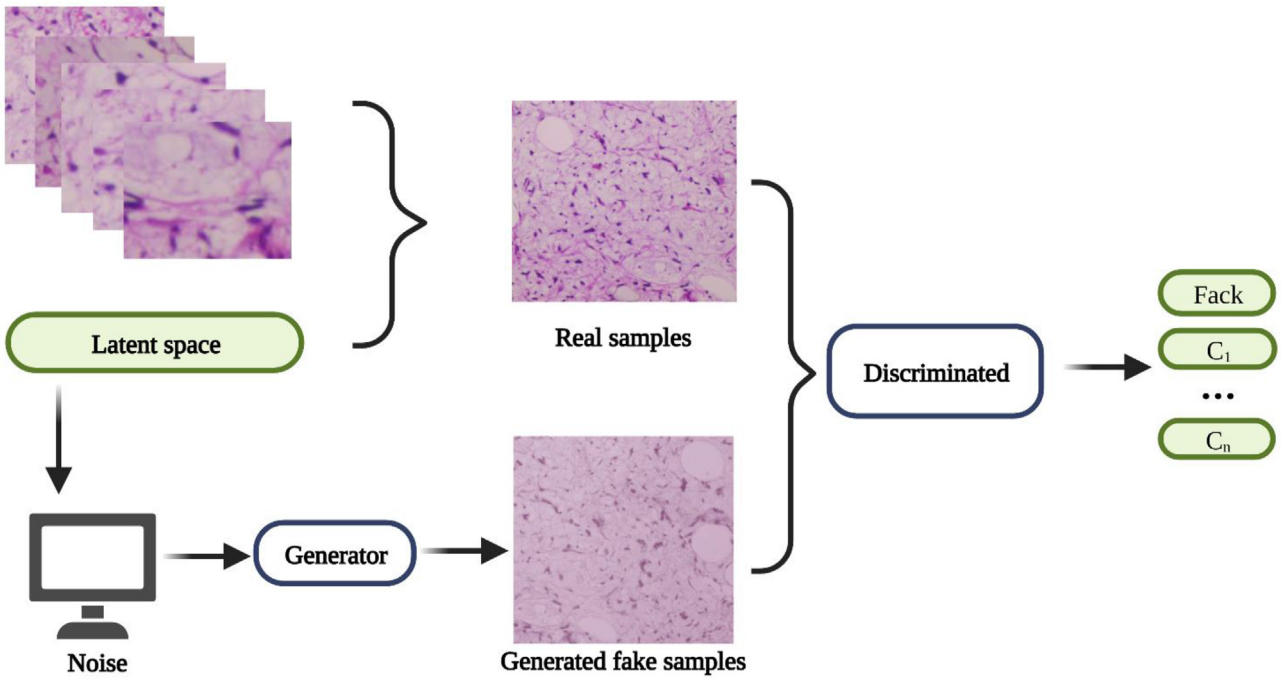

Fig. 4. Generative adversarial network (GAN)-based data augmentation.

metastases in STSs patients prior to surgery.[75] This study retrospectively enrolled 242 patients with STSs who underwent MRI. Handcrafted radiomics extracted 949 features from T1WI and 772 features from FS-T2WI, and DL extracted 54 parameters from T1WI and 50 features from FS-T2WI, which were used to construct the model. As compared to the clinical and radiomics models with the external validation set, the AUC value of DLRN model was the best (0.833).

Liposarcomas are common in STSs, and well-differentiated liposarcoma (WDLPS) accounts for the largest proportion, characterized by local aggressiveness and amplificatory MDM2 mutations.[4] In order to distinguish between WDLPS and lipoma (a benign lipomatous tumor), researchers constructed a prediction model using multimodal imaging with 127 patients, of which 89 underwent model training and 38 underwent external validation.[76] By manually analyzing radiomics, 851 features are extracted, whereas DL extracts 512–2048 features automatically. The clinical radiological model developed for WDLPS and lipoma identification was based on the combination of features and clinical factors. Based on the ResNet50 algorithm, a multimodal DL model was constructed. In external validation, the AUC, accuracy, sensitivity, and specificity reached 95.00%, 92.11%, and 88.89%, respectively. An external validation AUC of 0.942 was found in the comprehensive clinical radiology model. Taken together, the above studies have proved the feasibility and credibility of the combination of radiomics and DL. However, there are still many technical issues worthy of further exploration.

2.3.5. *Gene and pathway analysis*

Of note, in addition to conventional medical images, some researchers combined the genome profile with in-depth AI to explore tumor mechanisms and precision medicine.[124–128] Transcriptome sequencing data can be a valuable source to understand differences between and within entities by AI. The random forest algorithm was performed to promote novel diagnostic markers for STSs, and that was validated by qRT-PCR in an independent series. Recent studies attempted to adopt ML to identify differences between and within STSs using openly available expression data derived from STSs.[53] The more novel approach is to use DL to improve the previous bioinformatics methods to increase the credibility and accuracy of the results.

Recently, A DL model-dgMDL used deep belief networks (DBNs) to predict disease-gene associations.[129] Besides, Y Chen et al. also developed a multi-task multi-layer feedforward neural network that was capable of inferring gene expression data.[130] STSs are more strongly associated with epigenetic deregulation than other tumors.[131,132] Moreover, it is difficult to interpret DNA methylation patterns at the gene level, which hinders our understanding of their biological significance.[133] Accordingly, J Williams et al. developed MethylationToActivity that used CNNs for predicting promoter activities based on enrichment of H3K4me3 and H3K27ac from DNA methylation patterns.[133] As a result, it performed accurately, robustly, and with generalizability in a wide range of cancers including RMS.

In tumor diagnosis, circulating cell-free DNA (cfDNA) in peripheral blood is typically analyzed via liquid biopsy.[134] The presence of tumor-derived DNA in blood has been associated with clinical outcomes in pediatric tumors as well.[135] Currently, there has been emerging studies on ML to identify cfDNA biomarkers,[136,137] it may be possible to integrate DL model to further validate the diagnostic capacities of cfDNA in near future.

Pathway analysis is another important aspect in tumor research that has proven to be a useful technique for gaining insight into the processes underlying tumorigenesis. Recently, researchers proposed a stacked denoising autoencoder multi-label learning (SDaMLL) model to investigate the effects, if any, that gene multi-functions may have on cancer pathways in the Kyoto encyclopedia of genes and genomes (KEGG).[138]

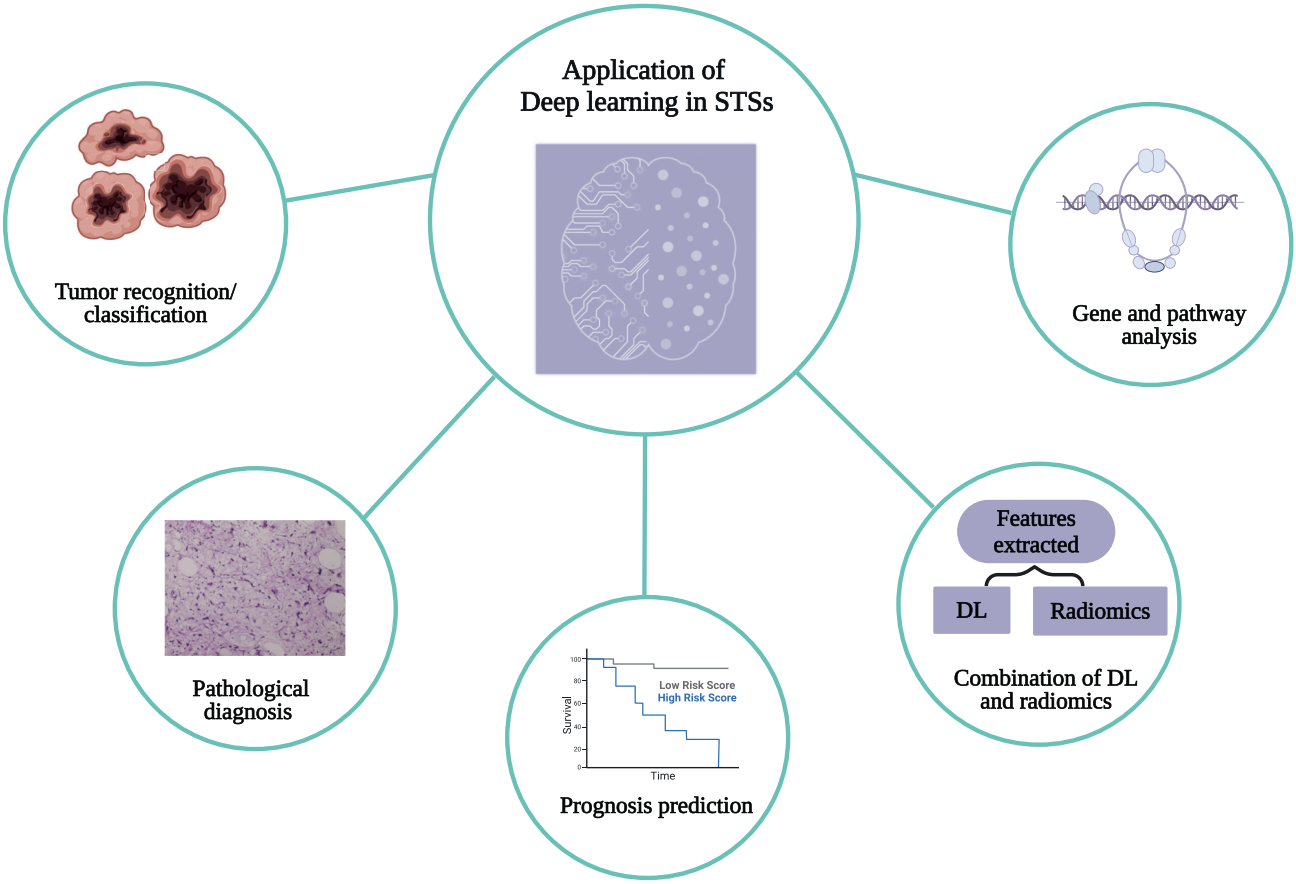

Fig. 5. Application of deep learning in STSs.

The results on eight KEGG cancer pathways revealed that SdaMLL was not only much better than classical multi-label learning models such as K-nearest neighbors and decision trees but can also function on a wide range of genes related to important cancer pathways.

To sum up, DL can participate in the screening of key genes and subsequent pathway analysis, which merits in-depth exploration.

3. Conclusions and perspectives

DL applications are rapidly emerging in STSs. Considering the examples of DL in STSs described above, the development and integration of DL systems in daily practice can bring about several benefits in tumor recognition and grading, pathological diagnosis, prognosis prediction, and gene analysis (Fig. 5). Nowadays, diagnostic, prognostic, and treatment of STSs face multiple challenges. Computational methods such as deep reinforcement learning, and DL may be able to help. First of all, accurate diagnosis and classification are the most critical step in the process of medicine. DL models have shown excellent diagnostic ability and more refined classification ability, which is very helpful to guide clinicians' follow-up treatment. Secondly, precision treatment is the core means. DL models can help guide the use of highly sensitive drugs and avoid the emergence of drug resistance. The application prospect is very attractive. Finally, the prediction of clinical outcomes is something clinicians and patients are keen to know, as it can be used to guide early clinical intervention. In this respect, DL models can obtain very accurate results by analyzing clinical data and image data.

It Is believed that the use of DL in conjunction with standard practices within radiology, pathology, and clinical parameters has the potential to improve the speed and accuracy of diagnostic testing while human resources are no longer required to perform time-consuming tasks due to offloading. Aside from that, DL systems are subject to some of the same pitfalls as human-based diagnoses, such as inter- and intra-observer variation. Academic research settings can benefit from DL, as it can at least match, and sometimes exceed, the performance of humans.

The orthopaedic surgeons, radiologist and pathologist are expected to play a leading role in ongoing discussions about how to utilize DL in clinical practice. With the development of DL and the increase of medical data, more STSs could be annotated and further explored in-depth.

However, because of the particularity of STSs, the number of patients and the corresponding data are much less than those of other tumors, which may introduce potential limitation of DL in training models in STSs. Thus, adapting a DL framework using transfer learning and data augmentation may be an alternative approach in STSs.

Besides, as DL models play an increasingly vital role in many medical scenarios, the interpretability of models is vital since it determines whether the clinicians can make decisions based on these models. To increase the reliability and transparency of the DL model, it is necessary to explain the prediction results of the DL model from the perspectives of interpretability and integrity. In conclusion, we should not only focus on the efficacy of the model, but also put emphasis on explanation of the underlying logic as well.

What's more, a comprehensive and comprehensible explanation of the medical condition to the patients is also necessary for a better STS treatment. In this field, artificial general intelligence (AGI) or large language models (LLMs) such as GPT4 from OpenAI have shown a great transformative potential. Leveraging public data, these models get remarkable language understanding and generation capabilities. By using LLMs to translate complex medical information into more understandable terms, patients can get a greater understanding of their own illness, while the doctors can also get greater interpretive skills. Especially in complex diseases like STS, LLMs will unleash their full potential.

Authorship Statement

Ruiling Xu: Writing – original draft, Visualization, Investigation, Conceptualization. **Jinxin Tang:** Writing – review & editing, Visualization. **Chenbei Li:** Writing – review & editing. **Hua Wang:** Writing – review & editing. **Lan Li:** Writing – review & editing. **Yu He:** Writing – review & editing. **Chao Tu:** Writing – review & editing, Supervision, Conceptualization. **Zhihong Li:** Writing – review & editing, Supervision, Conceptualization.

Declaration of interests

The authors declare that they have no known competing financial interests or personal relationships that could have appeared to influence the work reported in this paper. The Author Zhihong Li is the Editor-in-Chief of the journal, but was not involved in the peer review procedure. This paper was handled by another Editor Board member.

Acknowledgements

This work was supported by the National Natural Foundation of China (82272664, 81902745), Hunan Provincial Natural Science Foundation of China (2022JJ30843), the Science and Technology Development Fund Guided by Central Government (2021Szvup169), Hunan Provincial Administration of Traditional Chinese Medicine Project (D2022117), the Scientific Research Program of Hunan Provincial Health Commission (B202304077077), and the Science and Technology Innovation Program of Hunan Province (2023RC3085).

References

1. D'angelo S, Tap W, Schwartz G, Carvajal R. Sarcoma immunotherapy: past approaches and future directions. *Sarcoma*. 2014;2014. https://doi.org/10.1155/2014/391967.
2. Sharma S, Takyar S, Manson SC, Powell S, Penel N. Efficacy and safety of pharmacological interventions in second-or later-line treatment of patients with advanced soft tissue sarcoma: a systematic review. *BMC Cancer*. 2013;13:1–21. https://doi.org/10.1186/1471-2407-13-385.
3. Maki RG, D'Adamo DR, Keohan ML, et al. Phase II study of sorafenib in patients with metastatic or recurrent sarcomas. *J Clin Oncol*. 2009;27:3133–3140. https://doi.org/10.1200/jco.2008.20.4495.
4. Sbaraglia M, Bellan E, Dei Tos AP. The 2020 WHO classification of soft tissue tumours: news and perspectives. *Pathologica*. 2021;113:70–84. https://doi.org/10.32074/1591-951x-213.
5. Singer S, Demetri GD, Baldini EH, Fletcher CD. Management of soft-tissue sarcomas: an overview and update. *Lancet Oncol*. 2000;1:75–85. https://doi.org/10.1016/s1470-2045(00)00016-4.
6. Ryan C, Schoffski P, Merimsky O, et al. Picasso 3: a phase 3 international, randomized, double-blind, placebo-controlled study of doxorubicin (dox) plus palifosfamide (pali) vs. dox plus placebo for patients (pts) in first-line for metastatic soft tissue sarcoma (mSTS). *Eur J Cancer*. 2013;49:S876. https://doi.org/10.1200/JCO.2016.67.6684. S876.
7. Mutasa S, Varada S, Goel A, Wong TT, Rasiej MJ. Advanced deep learning techniques applied to automated femoral neck fracture detection and classification. *J Digit Imag*. 2020;33:1209–1217. https://doi.org/10.1007/s10278-020-00364-8.
8. Hoermann S, Bach M, Dietmayer KCJ. Dynamic occupancy grid prediction for urban autonomous driving: a deep learning approach with fully automatic labeling. *2018 IEEE International Conference on Robotics and Automation (ICRA)*. 2017: 2056–2063. https://doi.org/10.1109/ICRA.2018.8460874.
9. Hinton G, Deng L, Yu D, et al. Deep neural networks for acoustic modeling in speech recognition: the shared views of four research groups. *IEEE Signal Process Mag*. 2012;29:82–97. https://doi.org/10.1109/MSP.2012.2205597.
10. Collobert R, Weston J, Bottou L, Karlen M, Kavukcuoglu K, Kuksa P. Natural language processing (almost) from scratch. *J Mach Learn Res*. 2011;12: 2493−–2537. https://doi.org/10.48550/arXiv.1103.0398.
11. Bucci MA, Semeraro O, Allauzen A, Wisniewski G, Cordier L, Mathelin L. Control of chaotic systems by deep reinforcement learning. *Proceedings of the Royal Society A*. 2019;475:20190351. https://doi.org/10.1098/rspa.2019.0351.
12. Huang D-S, Zheng C-H. Independent component analysis-based penalized discriminant method for tumor classification using gene expression data. *Bioinformatics*. 2006;22:1855–1862. https://doi.org/10.1093/bioinformatics/btl190.
13. Chuai G, Ma H, Yan J, et al. DeepCRISPR: optimized CRISPR guide RNA design by deep learning. *Genome Biol*. 2018;19:1–18. https://doi.org/10.1186/s13059-018-1459-4.
14. Cicero M, Bilbily A, Colak E, et al. Training and validating a deep convolutional neural network for computer-aided detection and classification of abnormalities on frontal chest radiographs. *Invest Radiol*. 2017;52:281–287. https://doi.org/10.1097/rli.0000000000000341.
15. Kooi T, Litjens G, van Ginneken B, et al. Large scale deep learning for computer aided detection of mammographic lesions. *Med Image Anal*. 2017;35:303–312. https://doi.org/10.1016/j.media.2016.07.007.

16. Cheng JZ, Ni D, Chou YH, et al. Computer-Aided diagnosis with deep learning architecture: applications to breast lesions in US images and pulmonary nodules in CT scans. *Sci Rep*. 2016;6:24454. https://doi.org/10.1038/srep24454.
17. Tang H, Sun N, Shen S. Improving generalization of deep learning models for diagnostic pathology by increasing variability in training data: experiments on osteosarcoma subtypes. *J Pathol Inf*. 2021;12:30. https://doi.org/10.4103/jpi.jpi_78_20.
18. Hou L, Nguyen V, Kanevsky AB, et al. Sparse autoencoder for unsupervised nucleus detection and representation in histopathology images. *Pattern Recogn*. 2019;86:188–200. https://doi.org/10.1016/j.patcog.2018.09.007.
19. Li C, Wang X, Liu W, Latecki LJ. DeepMitosis: mitosis detection via deep detection, verification and segmentation networks. *Med Image Anal*. 2018;45:121–133. https://doi.org/10.1016/j.media.2017.12.002.
20. Kather JN, Pearson AT, Halama N, et al. Deep learning can predict microsatellite instability directly from histology in gastrointestinal cancer. *Nat Med*. 2019;25:1054–1056. https://doi.org/10.1038/s41591-019-0462-y.
21. Cho SY, Lee JH, Ryu JM, et al. Deep learning from HE slides predicts the clinical benefit from adjuvant chemotherapy in hormone receptor-positive breast cancer patients. *Sci Rep*. 2021;11:17363. https://doi.org/10.1038/s41598-021-96855-x.
22. Teplitzky BA, McRoberts M, Ghanbari H. Deep learning for comprehensive ECG annotation. *Heart Rhythm*. 2020;17:881–888. https://doi.org/10.1016/j.hrthm.2020.02.015.
23. Strodthoff N, Wagner P, Schaeffter T, Samek W. Deep learning for ECG analysis: benchmarks and insights from PTB-XL. *IEEE J Biomed Health Inform*. 2021;25:1519–1528. https://doi.org/10.1109/jbhi.2020.3022989.
24. Craik A, He Y, Contreras-Vidal JL. Deep learning for electroencephalogram (EEG) classification tasks: a review. *J Neural Eng*. 2019;16:031001. https://doi.org/10.1088/1741-2552/ab0ab5.
25. Zaharchuk G, Gong E, Wintermark M, Rubin D, Langlotz CP. Deep learning in neuroradiology. *AJNR Am J Neuroradiol*. 2018;39:1776–1784. https://doi.org/10.3174/ajnr.A5543.
26. Urakawa T, Tanaka Y, Goto S, Matsuzawa H, Watanabe K, Endo N. Detecting intertrochanteric hip fractures with orthopedist-level accuracy using a deep convolutional neural network. *Skeletal Radiol*. 2019;48:239–244. https://doi.org/10.1007/s00256-018-3016-3.
27. Adams M, Chen W, Holcdorf D, McCusker MW, Howe PD, Gaillard F. Computer vs human: deep learning versus perceptual training for the detection of neck of femur fractures. *J Med Imaging Radiat Oncol*. 2019;63:27–32. https://doi.org/10.1111/1754-9485.12828.
28. Tomita N, Cheung YY, Hassanpour S. Deep neural networks for automatic detection of osteoporotic vertebral fractures on CT scans. *Comput Biol Med*. 2018;98:8–15. https://doi.org/10.1016/j.compbiomed.2018.05.011.
29. Rifaioglu AS, Atas H, Martin MJ, Cetin-Atalay R, Atalay V, Doğan T. Recent applications of deep learning and machine intelligence on in silico drug discovery: methods, tools and databases. *Briefings Bioinf*. 2019;20:1878–1912. https://doi.org/10.1093/bib/bby061.
30. Araújo T, Aresta G, Castro E, et al. Classification of breast cancer histology images using Convolutional Neural Networks. *PLoS One*. 2017;12:e0177544. https://doi.org/10.1371/journal.pone.0177544.
31. Bejnordi BE, Zuidhof G, Balkenhol M, et al. Context-aware stacked convolutional neural networks for classification of breast carcinomas in whole-slide histopathology images. *J Med Imaging*. 2017;4:044504. https://doi.org/10.1117/1.Jmi.4.4.044504.
32. Teramoto A, Tsukamoto T, Kiriyama Y, Fujita H. Automated classification of lung cancer types from cytological images using deep convolutional neural networks. *BioMed Res Int*. 2017;2017:4067832. https://doi.org/10.1155/2017/4067832.
33. Aprupe L, Litjens G, Brinker TJ, van der Laak J, Grabe N. Robust and accurate quantification of biomarkers of immune cells in lung cancer micro-environment using deep convolutional neural networks. *PeerJ*. 2019;7:e6335. https://doi.org/10.7717/peerj.6335.
34. Kainz P, Pfeiffer M, Urschler M. Segmentation and classification of colon glands with deep convolutional neural networks and total variation regularization. *PeerJ*. 2017;5:e3874. https://doi.org/10.7717/peerj.3874.
35. Wang S, Zhu Y, Yu L, et al. RMDL: recalibrated multi-instance deep learning for whole slide gastric image classification. *Med Image Anal*. 2019;58:101549. https://doi.org/10.1016/j.media.2019.101549.
36. Arvaniti E, Fricker KS, Moret M, et al. Automated Gleason grading of prostate cancer tissue microarrays via deep learning. *Sci Rep*. 2018;8:12054. https://doi.org/10.1038/s41598-018-30535-1.
37. Zhang L, Le L, Nogues I, Summers RM, Liu S, Yao J. DeepPap: deep convolutional networks for cervical cell classification. *IEEE J Biomed Health Inform*. 2017;21:1633–1643. https://doi.org/10.1109/jbhi.2017.2705583.
38. Guan Q, Wang Y, Ping B, et al. Deep convolutional neural network VGG-16 model for differential diagnosing of papillary thyroid carcinomas in cytological images: a pilot study. *J Cancer*. 2019;10:4876–4882. https://doi.org/10.7150/jca.28769.
39. Eweje FR, Bao B, Wu J, et al. Deep learning for classification of bone lesions on routine MRI. *EBioMedicine*. 2021;68:103402. https://doi.org/10.1016/j.ebiom.2021.103402.
40. Foersch S, Eckstein M, Wagner DC, et al. Deep learning for diagnosis and survival prediction in soft tissue sarcoma. *Ann Oncol*. 2021;32:1178–1187. https://doi.org/10.1016/j.annonc.2021.06.007.
41. Siegel RL, Miller KD, Fuchs HE, Jemal A. Cancer statistics, 2021. *CA A Cancer J Clin*. 2021;71:7–33. https://doi.org/10.3322/caac.21654.
42. Toro JR, Travis LB, Wu HJ, Zhu K, Fletcher CD, Devesa SS. Incidence patterns of soft tissue sarcomas, regardless of primary site, in the surveillance, epidemiology and end results program, 1978-2001: an analysis of 26,758 cases. *Int J Cancer*. 2006;119:2922–2930. https://doi.org/10.1002/ijc.22239.
43. Pastore G, Peris-Bonet R, Carli M, Martínez-García C, Sánchez de Toledo J, Steliarova-Foucher E. Childhood soft tissue sarcomas incidence and survival in European children (1978-1997): report from the Automated Childhood Cancer Information System project. *Eur J Cancer*. 2006;42:2136–2149. https://doi.org/10.1016/j.ejca.2006.05.016.
44. Liu S, Sun W, Yang S, et al. Deep learning radiomic nomogram to predict recurrence in soft tissue sarcoma: a multi-institutional study. *Eur Radiol*. 2021. https://doi.org/10.1007/s00330-021-08221-0.
45. Wang Q, Kille B, Liu TR, Elworth RAL, Treangen TJ. PlasmidHawk improves lab of origin prediction of engineered plasmids using sequence alignment. *Nat Commun*. 2021;12:1167. https://doi.org/10.1038/s41467-021-21180-w.
46. Sinha S, Peach AH. Diagnosis and management of soft tissue sarcoma. *Bmj*. 2010;341:c7170. https://doi.org/10.1136/bmj.c7170.
47. Han I, Kim JH, Park H, Kim HS, Seo SW. Deep learning approach for survival prediction for patients with synovial sarcoma. *Tumour Biol*. 2018;40:1010428318799264. https://doi.org/10.1177/1010428318799264.
48. Peeken JC, Asadpour R, Specht K, et al. MRI-based delta-radiomics predicts pathologic complete response in high-grade soft-tissue sarcoma patients treated with neoadjuvant therapy. *Radiother Oncol*. 2021;164:73–82. https://doi.org/10.1016/j.radonc.2021.08.023.
49. Banerjee I, Crawley A, Bhethanabotla M, Daldrup-Link HE, Rubin DL. Transfer learning on fused multiparametric MR images for classifying histopathological subtypes of rhabdomyosarcoma. *Comput Med Imag Graph*. 2018;65:167–175. https://doi.org/10.1016/j.compmedimag.2017.05.002.
50. Gao Y, Ghodrati V, Kalbasi A, et al. Prediction of soft tissue sarcoma response to radiotherapy using longitudinal diffusion MRI and a deep neural network with generative adversarial network-based data augmentation. *Med Phys*. 2021;48:3262–3372. https://doi.org/10.1002/mp.14897.
51. Navarro F, Dapper H, Asadpour R, et al. Development and external validation of deep-learning-based tumor grading models in soft-tissue sarcoma patients using MR imaging. *Cancers*. 2021;13. https://doi.org/10.3390/cancers13122866.
52. Ye Y, Sun WW, Xu RX, Selmic LE, Sun M. Intraoperative assessment of canine soft tissue sarcoma by deep learning enhanced optical coherence tomography. *Vet Comp Oncol*. 2021;19:624–631. https://doi.org/10.1111/vco.12747.
53. van IDGP, Szuhai K, Briaire-de Bruijn IH, Kostine M, Kuijjer ML, Bovee J. Machine learning analysis of gene expression data reveals novel diagnostic and prognostic biomarkers and identifies therapeutic targets for soft tissue sarcomas. *PLoS Comput Biol*. 2019;15:e1006826. https://doi.org/10.1371/journal.pcbi.1006826.
54. Ryu SM, Seo SW, Lee SH. Novel prognostication of patients with spinal and pelvic chondrosarcoma using deep survival neural networks. *BMC Med Inf Decis Making*. 2020;20:3. https://doi.org/10.1186/s12911-019-1008-4.
55. Bhambhvani HP, Zamora A, Velaer K, Greenberg DR, Sheth KR. Deep learning enabled prediction of 5-year survival in pediatric genitourinary rhabdomyosarcoma. *Surg Oncol*. 2021;36:23–27. https://doi.org/10.1016/j.suronc.2020.11.002.
56. Zhao W, Zhang W, Sun Y, et al. Convolution kernel and iterative reconstruction affect the diagnostic performance of radiomics and deep learning in lung adenocarcinoma pathological subtypes. *Thorac Cancer*. 2019;10:1893–1903. https://doi.org/10.1111/1759-7714.13161.
57. Wang S, Yang DM, Rong R, Zhan X, Xiao G. Pathology image analysis using segmentation deep learning algorithms. *Am J Pathol*. 2019;189:1686–1698. https://doi.org/10.1016/j.ajpath.2019.05.007.
58. Philbrick KA, Weston AD, Akkus Z, et al. RIL-contour: a medical imaging dataset annotation tool for and with deep learning. *J Digit Imag*. 2019;32:571–581. https://doi.org/10.1007/s10278-019-00232-0.
59. Yu S, Chen M, Zhang E, et al. Robustness study of noisy annotation in deep learning based medical image segmentation. *Phys Med Biol*. 2020;65:175007. https://doi.org/10.1088/1361-6560/ab99e5.
60. Lucas AM, Ryder PV, Li B, Cimini BA, Eliceiri KW, Carpenter AE. Open-source deep-learning software for bioimage segmentation. *Mol Biol Cell*. 2021;32:823–829. https://doi.org/10.1091/mbc.E20-10-0660.
61. Angehrn Z, Haldna L, Zandvliet AS, et al. Artificial intelligence and machine learning applied at the point of care. *Front Pharmacol*. 2020;11:759. https://doi.org/10.3389/fphar.2020.00759.
62. Yamamoto Y, Tsuzuki T, Akatsuka J, et al. Automated acquisition of explainable knowledge from unannotated histopathology images. *Nat Commun*. 2019;10:5642. https://doi.org/10.1038/s41467-019-13647-8.
63. Hunter B, Hindocha S, Lee RW. The role of artificial intelligence in early cancer diagnosis. *Cancers*. 2022;14. https://doi.org/10.3390/cancers14061524.
64. Sánchez-Corrales YE, Pohle RVC, Castellano S, Giustacchini A. Taming cell-to-cell heterogeneity in acute myeloid leukaemia with machine learning. *Front Oncol*. 2021;11:666829. https://doi.org/10.3389/fonc.2021.666829.
65. Ajani TS, Imoize AL, Atayero AA. An overview of machine learning within embedded and mobile devices-optimizations and applications. *Sensors*. 2021;21. https://doi.org/10.3390/s21134412.
66. Yang B, Xu Y. Applications of deep-learning approaches in horticultural research: a review. *Hortic Res*. 2021;8:123. https://doi.org/10.1038/s41438-021-00560-9.
67. LeCun Y, Bottou L, Bengio Y, Haffner P. Gradient-based learning applied to document recognition. *Proc IEEE*. 1998;86:2278–2324. https://doi.org/10.1109/5.726791.
68. Going deeper with convolutions. In: Szegedy C, Liu W, Jia Y, et al., eds. *Proceedings of the IEEE Conference on Computer Vision and Pattern Recognition*. 2015.

69. Simonyan K, Zisserman A. Very deep convolutional networks for large-scale image recognition. *arXiv preprint arXiv*. 2014:14091556.
70. Deep residual learning for image recognition. In: He K, Zhang X, Ren S, Sun J, eds. *Proceedings of the IEEE Conference on Computer Vision and Pattern Recognition*. 2016.
71. Densely connected convolutional networks. In: Huang G, Liu Z, Van Der Maaten L, Weinberger KQ, eds. *Proceedings of the IEEE Conference on Computer Vision and Pattern Recognition*. 2017.
72. Krizhevsky A, Sutskever I, Hinton GE. ImageNet classification with deep convolutional neural networks. *Commun ACM*. 2017;60:84–90. https://doi.org/10.1145/3065386.
73. He K, Zhang X, Ren S, Sun J. *Deep Residual Learning for Image Recognition*. IEEE; 2016.
74. Jardim-Perassi BV, Mu W, Huang S, et al. Deep-learning and MR images to target hypoxic habitats with evofosfamide in preclinical models of sarcoma. *Theranostics*. 2021;11:5313–5329. https://doi.org/10.7150/thno.56595.
75. Liang HY, Yang SF, Zou HM, et al. Deep learning radiomics nomogram to predict lung metastasis in soft-tissue sarcoma: a multi-center study. *Front Oncol*. 2022;12:897676. https://doi.org/10.3389/fonc.2022.897676.
76. Yang Y, Zhou Y, Zhou C, Ma X. Novel computer aided diagnostic models on multimodality medical images to differentiate well differentiated liposarcomas from lipomas approached by deep learning methods. *Orphanet J Rare Dis*. 2022;17:158. https://doi.org/10.1186/s13023-022-02304-x.
77. Ronneberger O, Fischer P, Brox T, eds. U-net: Convolutional Networks for Biomedical Image Segmentation2015; Cham: Springer International Publishing.
78. Holbrook MD, Blocker SJ, Mowery YM, et al. MRI-based deep learning segmentation and radiomics of sarcoma in mice. *Tomography*. 2020;6:23–33. https://doi.org/10.18383/j.tom.2019.00021.
79. U-net: convolutional networks for biomedical image segmentation. In: Ronneberger O, Fischer P, Brox T, eds. *International Conference on Medical Image Computing and Computer-Assisted Intervention*. Springer; 2015.
80. Rethinking the inception architecture for computer vision. In: Szegedy C, Vanhoucke V, Ioffe S, Shlens J, Wojna Z, eds. *Proceedings of the IEEE Conference on Computer Vision and Pattern Recognition*. 2016.
81. Ren S, He K, Girshick R, Sun J, Faster R-CNN. Towards real-time object detection with region proposal networks. *IEEE Trans Pattern Anal Mach Intell*. 2017;39:1137–1149. https://doi.org/10.1109/tpami.2016.2577031.
82. Wang X, Hua X, Xiao F, Li Y, Hu X, Sun P. Multi-object detection in traffic scenes based on improved SSD. *Electronics*. 2018;7:302. https://doi.org/10.3390/electronics7110302.
83. Ge Z, Liu S, Wang F, Li Z, Sun J. Yolox: exceeding yolo series in 2021. *arXiv preprint arXiv*. 2021:210708430.
84. YOLO v4 based human detection system using aerial thermal imaging for uav based surveillance applications. In: Kannadaguli P, ed. *2020 International Conference on Decision Aid Sciences and Application (DASA)*. IEEE; 2020.
85. Nersisson R, Iyer TJ, Joseph Raj AN, Rajangam V. A dermoscopic skin lesion classification technique using YOLO-CNN and traditional feature model. *Arabian J Sci Eng*. 2021;46:9797–9808. https://doi.org/10.1007/s13369-021-05571-1.
86. Yu J, Zhang W. Face mask wearing detection algorithm based on improved YOLO-v4. *Sensors*. 2021;21:3263. https://doi.org/10.3390/s21093263.
87. Gutierrez JC, Perez EA, Franceschi D, Moffat Jr FL, Livingstone AS, Koniaris LG. Outcomes for soft-tissue sarcoma in 8249 cases from a large state cancer registry. *J Surg Res*. 2007;141:105–114. https://doi.org/10.1016/j.jss.2007.02.026.
88. Edge SB, Compton CC. The American Joint Committee on Cancer: the 7th edition of the AJCC cancer staging manual and the future of TNM. *Ann Surg Oncol*. 2010;17:1471–1474. https://doi.org/10.1245/s10434-010-0985-4.
89. Plekhanova E, Nuzhdin SV, Utkin LV, Samsonova MG. Prediction of deleterious mutations in coding regions of mammals with transfer learning. *Evol Appl*. 2019;12:18–28. https://doi.org/10.1111/eva.12607.
90. Wang D, Zhang Q, Eisenberg BL, et al. Significant reduction of late toxicities in patients with extremity sarcoma treated with image-guided radiation therapy to a reduced target volume: results of radiation therapy oncology group RTOG-0630 trial. *J Clin Oncol*. 2015;33:2231. https://doi.org/10.1200/JCO.2014.58.5828.
91. Ng SP, Dyer BA, Kalpathy-Cramer J, et al. A prospective in silico analysis of interdisciplinary and interobserver spatial variability in post-operative target delineation of high-risk oral cavity cancers: does physician specialty matter? *Clinical and translational radiation oncology*. 2018;12:40–46. https://doi.org/10.1016/j.ctro.2018.07.006.
92. Anderson CM, Sun W, Buatti JM, et al. Interobserver and intermodality variability in GTV delineation on simulation CT, FDG-PET, and MR images of head and neck cancer. *Jacobs journal of radiation oncology*. 2014;1:6.
93. Guo Z, Guo N, Gong K, Zhong S, Li Q. Gross tumor volume segmentation for head and neck cancer radiotherapy using deep dense multi-modality network. *Phys Med Biol*. 2019;64:205015. https://doi.org/10.1088/1361-6560/ab440d.
94. Fischer AH, Jacobson KA, Rose J, Zeller R. Hematoxylin and eosin staining of tissue and cell sections. *CSH Protoc*. 2008;2008:prot4986. https://doi.org/10.1101/pdb.prot4986.
95. Yue X, Dimitriou N, Arandjelovic O. Colorectal cancer outcome prediction from H&E whole slide images using machine learning and automatically inferred phenotype profiles. *arXiv preprint arXiv*. 2019:190203582.
96. Wang D, Khosla A, Gargeya R, Irshad H, Beck AH. Deep learning for identifying metastatic breast cancer. *arXiv preprint arXiv*. 2016:160605718.
97. Liu Y, Gadepalli K, Norouzi M, et al. Detecting cancer metastases on gigapixel pathology images. *arXiv preprint arXiv*. 2017:170302442.
98. Lucas M, Jansen I, Savci-Heijink CD, et al. Deep learning for automatic Gleason pattern classification for grade group determination of prostate biopsies. *Virchows Arch*. 2019;475:77–83. https://doi.org/10.1007/s00428-019-02577-x.
99. Ries LAG. *Cancer Incidence and Survival Among Children and Adolescents: United States SEER Program, 1975-1995*. National Cancer Institute; 1999.
100. Rudzinski ER, Kelsey A, Vokuhl C, et al. Pathology of childhood rhabdomyosarcoma: a consensus opinion document from the children's oncology group, European paediatric soft tissue sarcoma study group, and the cooperative weichteilsarkom studiengruppe. *Pediatr Blood Cancer*. 2021;68:e28798. https://doi.org/10.1002/pbc.28798.
101. Newton Jr WA, Gehan EA, Webber BL, et al. Classification of rhabdomyosarcomas and related sarcomas. Pathologic aspects and proposal for a new classification-an intergroup rhabdomyosarcoma study. *Cancer*. 1995;76:1073–1085. https://doi.org/10.1002/1097-0142(19950915)76:6<1073::aid-cncr2820760624>3.0.co;2-l.
102. Zhang X, Wang S, Rudzinski ER, et al. Deep learning of rhabdomyosarcoma pathology images for classification and survival outcome prediction. *Am J Pathol*. 2022;192:917–925. https://doi.org/10.1016/j.ajpath.2022.03.011.
103. Frankel AO, Lathara M, Shaw CY, et al. Machine learning for rhabdomyosarcoma histopathology. *Mod Pathol*. 2022. https://doi.org/10.1038/s41379-022-01075-x.
104. Roberts ME, Aynardi JT, Chu CS. Uterine leiomyosarcoma: a review of the literature and update on management options. *Gynecol Oncol*. 2018;151:562–572. https://doi.org/10.1016/j.ygyno.2018.09.010.
105. Bell SW, Kempson RL, Hendrickson MR. Problematic uterine smooth muscle neoplasms. A clinicopathologic study of 213 cases. *Am J Surg Pathol*. 1994;18:535–558.
106. Zehra T, Anjum S, Mahmood T, et al. A novel deep learning-based mitosis recognition approach and dataset for uterine leiomyosarcoma. *Histopathology. Cancers (Basel)*. 2022;14. https://doi.org/10.3390/cancers14153785.
107. Borowitz MJ, Wood BL, Devidas M, et al. Prognostic significance of minimal residual disease in high risk B-ALL: a report from Children's Oncology Group study AALL0232. *Blood*. 2015;126:964–971. https://doi.org/10.1182/blood-2015-03-633685.
108. Mishra R, Daescu O, Leavey P, Rakheja D, Sengupta A. Convolutional neural network for histopathological analysis of osteosarcoma. *J Comput Biol*. 2018;25:313–325. https://doi.org/10.1089/cmb.2017.0153.
109. Wilson WR, Hay MP. Targeting hypoxia in cancer therapy. *Nat Rev Cancer*. 2011;11:393–410. https://doi.org/10.1038/nrc3064.
110. Liebner DA. The indications and efficacy of conventional chemotherapy in primary and recurrent sarcoma. *J Surg Oncol*. 2015;111:622–631. https://doi.org/10.1002/jso.23866.
111. Tap WD, Papai Z, Van Tine BA, et al. Doxorubicin plus evofosfamide versus doxorubicin alone in locally advanced, unresectable or metastatic soft-tissue sarcoma (TH CR-406/SARC021): an international, multicentre, open-label, randomised phase 3 trial. *Lancet Oncol*. 2017;18:1089–1103. https://doi.org/10.1016/s1470-2045(17)30381-9.
112. Koshino K, Werner RA, Pomper MG, et al. Narrative review of generative adversarial networks in medical and molecular imaging. *Ann Transl Med*. 2021;9:821. https://doi.org/10.21037/atm-20-6325.
113. Zhang Y, Lian H, Yang G, et al. Inaccurate-supervised learning with generative adversarial nets. *IEEE Trans Cybern*. 2021. https://doi.org/10.1109/tcyb.2021.3104848.
114. Jin CB, Kim H, Liu M, et al. Deep CT to MR synthesis using paired and unpaired data. *Sensors*. 2019;19. https://doi.org/10.3390/s19102361.
115. Costa P, Galdran A, Meyer MI, et al. End-to-End adversarial retinal image synthesis. *IEEE Trans Med Imag*. 2018;37:781–791. https://doi.org/10.1109/tmi.2017.2759102.
116. Sadda P, Qarni T. Real-time medical video denoising with deep learning: application to angiography. *Int J Appl Inf Syst*. 2018;12:22–28. https://doi.org/10.5120/ijais2018451755.
117. Stoyanov D, Taylor Z, Sarikaya D, et al. OR 2.0 context-aware operating theaters, computer assisted robotic endoscopy, clinical image-based procedures, and skin image analysis: first international workshop, OR 2.0 2018. In: *5th International Workshop, CARE 2018, 7th International Workshop, CLIP 2018, Third International Workshop, ISIC 2018, Held in Conjunction with MICCAI 2018*. Granada, Spain: Springer; 2018. September 16 and 20, 2018, Proceedings.
118. England JR, Gross JS, White EA, Patel DB, England JT, Cheng PM. Detection of traumatic pediatric elbow joint effusion using a deep convolutional neural network. *AJR Am J Roentgenol*. 2018;211:1361–1368. https://doi.org/10.2214/ajr.18.19974.
119. Chedid N, Sadda P, Gonchigar A, et al. Synthesis of fracture radiographs with deep neural networks. *Health Inf Sci Syst*. 2020;8:21. https://doi.org/10.1007/s13755-020-00111-x.
120. Ran J, Cao R, Cai J, Yu T, Zhao D, Wang Z. Development and validation of a nomogram for preoperative prediction of lymph node metastasis in lung adenocarcinoma based on radiomics signature and deep learning signature. *Front Oncol*. 2021;11:585942. https://doi.org/10.3389/fonc.2021.585942.
121. Caruso D, Polici M, Zerunian M, et al. Radiomics in oncology, Part 1: technical principles and gastrointestinal application in CT and MRI. *Cancers*. 2021;13. https://doi.org/10.3390/cancers13112522.
122. Yang Y, Zhou Y, Zhou C, Zhang X, Ma X. MRI-based computer-aided diagnostic model to predict tumor grading and clinical outcomes in patients with soft tissue sarcoma. *J Magn Reson Imag*. 2022. https://doi.org/10.1002/jmri.28160.
123. Brennan MF, Casper ES, Harrison LB, Shiu M, Gaynor J, Hajdu SI. The role of multimodality therapy in soft-tissue sarcoma. *Ann Surg*. 1991;214:328. https://doi.org/10.1097/00000658-199109000-00015.
124. Sørlie T, Perou CM, Tibshirani R, et al. Gene expression patterns of breast carcinomas distinguish tumor subclasses with clinical implications. *Proc Natl Acad Sci U S A*. 2001;98:10869–10874. https://doi.org/10.1073/pnas.191367098.

125. Lu J, Getz G, Miska EA, et al. MicroRNA expression profiles classify human cancers. *Nature*. 2005;435:834–838. https://doi.org/10.1038/nature03702.
126. Röhrich M, Koelsche C, Schrimpf D, et al. Methylation-based classification of benign and malignant peripheral nerve sheath tumors. *Acta Neuropathol*. 2016;131:877–887. https://doi.org/10.1007/s00401-016-1540-6.
127. Holder LB, Haque MM, Skinner MK. Machine learning for epigenetics and future medical applications. *Epigenetics*. 2017;12:505–514. https://doi.org/10.1080/15592294.2017.1329068.
128. Koh PW, Pierson E, Kundaje A. Denoising genome-wide histone ChIP-seq with convolutional neural networks. *Bioinformatics*. 2017;33:i225–i233. https://doi.org/10.1093/bioinformatics/btx243.
129. Li C, Liu H, Hu Q, Que J, Yao J. A novel computational model for predicting microRNA-disease associations based on heterogeneous graph convolutional networks. *Cells*. 2019;8. https://doi.org/10.3390/cells8090977.
130. Chen Y, Li Y, Narayan R, Subramanian A, Xie X. Gene expression inference with deep learning. *Bioinformatics*. 2016;32:1832–1839. https://doi.org/10.1093/bioinformatics/btw074.
131. Ma X, Liu Y, Liu Y, et al. Pan-cancer genome and transcriptome analyses of 1,699 paediatric leukaemias and solid tumours. *Nature*. 2018;555:371–376. https://doi.org/10.1038/nature25795.
132. Huether R, Dong L, Chen X, et al. The landscape of somatic mutations in epigenetic regulators across 1,000 paediatric cancer genomes. *Nat Commun*. 2014;5:1–7. https://doi.org/10.1038/ncomms4630.
133. Williams J, Xu B, Putnam D, et al. MethylationToActivity: a deep-learning framework that reveals promoter activity landscapes from DNA methylomes in individual tumors. *Genome Biol*. 2021;22:24. https://doi.org/10.1186/s13059-020-02220-y.
134. Corcoran RB, Chabner BA. Application of cell-free DNA analysis to cancer treatment. *N Engl J Med*. 2018;379:1754–1765. https://doi.org/10.1056/NEJMra1706174.
135. Shulman DS, Klega K, Imamovic-Tuco A, et al. Detection of circulating tumour DNA is associated with inferior outcomes in Ewing sarcoma and osteosarcoma: a report from the Children's Oncology Group. *Br J Cancer*. 2018;119:615–621. https://doi.org/10.1038/s41416-018-0212-9.
136. Peneder P, Stütz AM, Surdez D, et al. Multimodal analysis of cell-free DNA whole-genome sequencing for pediatric cancers with low mutational burden. *Nat Commun*. 2021;12:3230. https://doi.org/10.1038/s41467-021-23445-w.
137. Pastuszak K, Supernat A, Best MG, et al. imPlatelet classifier: image-converted RNA biomarker profiles enable blood-based cancer diagnostics. *Mol Oncol*. 2021;15:2688–2701. https://doi.org/10.1002/1878-0261.13014.
138. Guan R, Wang X, Yang MQ, et al. Multi-label deep learning for gene function annotation in cancer pathways. *Sci Rep*. 2018;8:267. https://doi.org/10.1038/s41598-017-17842-9.
139. Peng Y, Bi L, Guo Y, Feng D, Fulham M, Kim J. Deep multi-modality collaborative learning for distant metastases predication in PET-CT soft-tissue sarcoma studies. *Annu Int Conf IEEE Eng Med Biol Soc*. 2019;2019:3658–3688. https://doi.org/10.1109/embc.2019.8857666.
140. Marin T, Zhuo Y, Lahoud RM, et al. Deep learning-based GTV contouring modeling inter- and intra- observer variability in sarcomas. *Radiother Oncol*. 2022;167:269–276. https://doi.org/10.1016/j.radonc.2021.09.034.